Arch. Mech., **69**, 2, pp. 105–130, Warszawa 2017

# Free vibration analysis of functionally graded rectangular nanoplates considering spatial variation of the nonlocal parameter

A. ALIPOUR GHASSABI, S. DAG, E. CIGEROGLU

*Department of Mechanical Engineering*
*Middle East Technical University*
*Ankara 06800, Turkey*
*e-mail: sdag@metu.edu.tr*

We present a new nonlocal elasticity-based analysis method for free vibrations of functionally graded rectangular nanoplates. The introduced method allows taking into account spatial variation of the nonlocal parameter. Governing partial differential equations and associated boundary conditions are derived by employing the variational approach and applying Hamilton's principle. Displacement field is expressed in a unified way to be able to produce numerical results pertaining to three different plate theories, namely Kirchhoff, Mindlin, and third-order shear deformation theories. The equations are solved numerically by means of the generalized differential quadrature method. Numerical results are generated by considering simply-supported and cantilever nanoplates undergoing free vibrations. These findings demonstrate the influences of factors such as dimensionless plate length, plate theory, power-law index, and nonlocal parameter ratio upon vibration behavior.

**Key words:** functionally graded materials, nanoplates, nonlocal elasticity, differential quadrature method, free vibrations.



## 1. Introduction

Functionally graded materials (FGMs) are a special class of composites, which possess smooth spatial variations in the volume fractions of the constituent phases. FGMs find applications in a wide variety of technological fields including thermal barrier coatings, solid oxide fuel cells, high performance cutting tools, and biomedical materials. Deployment of functionally graded components in small-scale systems has recently become feasible with advances in fabrication technologies such as magnetron sputtering [1], chemical vapor deposition and plasma enhanced chemical vapor deposition [2], and modified soft lithography [3]. These developments are accompanied by theoretical and computational studies directed toward understanding the mechanical behavior of small-scale FGM composite structures. Classical continuum theories fail to account for the size effect observable at small-scales, whereas molecular dynamics-based simu-

lations need to confront an immense computational effort. As a result, higher order continuum theories have been used to examine the behavior of small-scale FGM beams, plates, and shells. Among such theories, we can mention nonlocal elasticity [4, 5], strain gradient elasticity [6–9], and couple stress theories [10–12].

The nonlocal elasticity theory has been widely used to investigate small-scale effects on free vibrations, bending and buckling of functionally graded beams and plates. Works on functionally graded nonlocal beams encompass free vibrations [13, 14], buckling [15,16], nonlinear vibrations [17], surface effects [18], forced vibrations [19], and thermomechanical vibrations [20]. Finite element analysis-based solutions are presented by Eltaher *et al.* [21–23] and Reddy *et al.* [24]. Studies pertaining to nonlocal FGM plates consider free vibrations [25–28], buckling [29, 30], effect of distributed nanoparticles [31] and the Winkler–Pasternak elastic foundation [32]. Novel three-dimensional (3D) modelling and analysis techniques are described by Salehipour *et al.* [33] and Ansari *et al.* [34].

Isogeometric analysis [35], which offers an exact geometry representation through the CAD modelling tool called non-uniform rational B-splines (NURBS) and is implemented in a finite element analysis setting, was also employed to solve structural mechanics problems involving nonlocal FGM plates. Natarajan *et al.* [36] examined free vibrations of functionally graded nanoplates by using isogeometric analysis in conjunction with finite element method. Nguyen *et al.* [37] developed the isogeometric analysis-based quasi-3D solution strategies for bending, vibration, and buckling of nonlocal graded plates. An application involving buckling of graded nanoplates is presented by Ansari and Norouzzadeh [38]. Theory and implementation of the method for macro-scale analysis of FGM components can be found in [39–41].

In a nonlocal elasticity-based formulation, in addition to the elastic properties, a material property called nonlocal parameter is required. The nonlocal parameter depends on both internal characteristic length and the material, thus it is essentially a material property [42]. In a functionally graded medium, all material properties vary smoothly from one bounding surface to the other. Since the nonlocal parameter is a material property, it should also possess a smooth spatial variation throughout the functionally graded medium. However, in all research work employing nonlocal elasticity cited in the foregoing paragraphs, the nonlocal parameter is assumed to be a constant. There are research studies accounting for the spatial variation of the length scale parameter of modified couple stress theory [12, 43, 44]. But, there is no nonlocal elasticity-based previous work taking into account spatial variation of the nonlocal parameter. Nonlocal elasticity and modified couple stress theory are built upon completely different constitutive relationships and deformation measures. Nonlocal elasticity is applied for problems involving nanoscale structures, whereas modified couple stress theory is employed for microscale problems. Thus, new developments considering

spatial variation of the nonlocal parameter are needed for more realistic nonlocal elasticity-based modeling of functionally graded small-scale structures. Furthermore, in the previous work on variable length scale parameter, beams [43] and circular plates [12, 44] were examined. There is no investigation on the spatial variation of length scale parameter or nonlocal parameter of rectangular plate geometries.

The primary objective in the present study is to put forward a free vibration analysis method capable of accounting for the *spatial variation of the nonlocal parameter*. The novel aspects of the article are therefore consideration of spatial variation of the nonlocal parameter in nonlocal elasticity of FGMs, and treatment of a nanoscale FGM rectangular plate possessing this nonlocal parameter variation. The presented numerical results could be useful as benchmarks for future work on vibrations of nanoscale functionally graded rectangular plates.

In the formulation, a set of governing partial differential equations and boundary conditions are derived by employing the nonlocal elasticity theory and variational principles. All material properties, including the nonlocal parameter, are assumed to be functions of the thickness coordinate. Displacement field is expressed in a unified way to be able to produce numerical results for three different plate theories: Kirchhoff, Mindlin, and third-order plate theories. Simply-supported and cantilever nanoplates are considered to specify the boundary conditions. The equations are solved numerically by means of a generalized differential quadrature method. Findings available in the literature for constant nonlocal parameter are used to verify the developed procedures. The presented numerical results illustrate in a clear way the impacts of nonlocal parameter variation and other related factors on free vibration behavior of rectangular FGM nanoplates.

## 2. Formulation

Figure 1 depicts a functionally graded rectangular nanoplate. The plate is of thickness $h$ and assumed to possess material property variations in $z$-direction. In the nonlocal elasticity theory, stress at a point is expressed as a function of the strain field in the material domain as follows:

$$\sigma_{ij} = \iiint_V \alpha(|x' - x|, \tau) t_{ij}(x')\, dV(x'), \tag{2.1}$$

where $\alpha$ is a nonlocal modulus or the kernel function, $|x' - x|$ represents distance, $\tau$ is a material property that depends on internal and external characteristic lengths (such as lattice spacing and wavelength), and $\sigma_{ij}$ and $t_{ij}$ stand

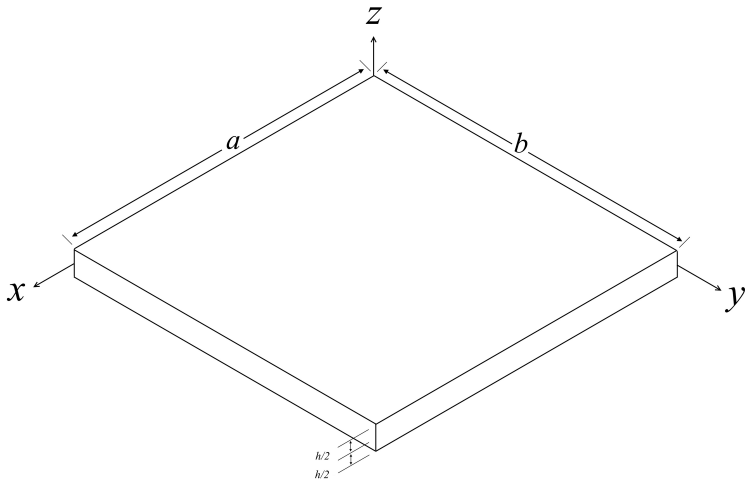


Fig. 1. A functionally graded rectangular nanoplate.

for nonlocal and local stress tensors, respectively. Eringen [45] proposed an equivalent differential form of the nonlocal constitutive equation in the form:

$$(1-\mu\nabla^2)\sigma_{ij} = t_{ij}, \tag{2.2}$$

$\mu$ in this equation is the nonlocal parameter defined by

$$\mu = (e_0 l)^2, \tag{2.3}$$

where $l$ is an internal characteristic length and $e_0$ is a material property found through experimental characterization. Because of its dependence on $l$ and $e_0$, $\mu$ is a material property. Thus, for a functionally graded small-scale plate, the nonlocal parameter $\mu$ should be a function of the thickness coordinate $z$.

The relation between the local stress tensor $t_{ij}$ and strain tensor $\varepsilon_{ij}$ is expressed by

$$\begin{Bmatrix} t_{xx} \\ t_{yy} \\ t_{xy} \\ t_{xz} \\ t_{yz} \end{Bmatrix} = \begin{pmatrix} Q_{11} & Q_{12} & 0 & 0 & 0 \\ Q_{21} & Q_{22} & 0 & 0 & 0 \\ 0 & 0 & Q_{66} & 0 & 0 \\ 0 & 0 & 0 & Q_{66} & 0 \\ 0 & 0 & 0 & 0 & Q_{66} \end{pmatrix} \begin{Bmatrix} \varepsilon_{xx} \\ \varepsilon_{yy} \\ 2\varepsilon_{xy} \\ 2\varepsilon_{xz} \\ 2\varepsilon_{yz} \end{Bmatrix}, \tag{2.4}$$

where

$$Q_{11} = Q_{22} = \frac{E(z)}{1-\nu(z)^2}, \quad Q_{12} = Q_{21} = \frac{E(z)\upsilon(z)}{1-\nu(z)^2}, \quad Q_{66} = \frac{E(z)}{2(1+\nu(z))}. \tag{2.5}$$

$E$ and $\nu$ are respectively modulus of elasticity and Poisson's ratio. All material properties including the nonlocal parameter are functions of the thickness coordinate and their spatial variations are described by

$$E(z) = E_c V_c(z) + E_m V_m(z), \qquad \nu(z) = \nu_c V_c(z) + \nu_m V_m(z), \tag{2.6}$$

$$\rho(z) = \rho_c V_c(z) + \rho_m V_m(z), \qquad \mu(z) = \mu_c V_c(z) + \mu_m V_m(z). \tag{2.7}$$

The subscripts $c$ and $m$ stand for ceramic and metallic phases; $V_c$ and $V_m$ are volume fractions; and $\rho$ in Eq. (2.7) is mass density. Spatial variations of the volume fractions are represented as follows:

$$V_c(z) = \left(\frac{1}{2} + \frac{z}{h}\right)^n, \qquad V_m(z) = 1 - V_c(z). \tag{2.8}$$

The power-law index $n$ defines property distribution profiles. When $n$ is less than 1, the nanoplate is ceramic-rich, whereas if $n$ is greater than unity, plate has a metal-rich FGM profile.

Currently, an approach suggested in the literature to determine the nonlocal parameter of a material is to carry out free vibration simulations by means of nonlocal elasticity and molecular dynamics, and adjust the nonlocal parameter to match the natural frequencies computed by these two methods [46–49]. For example, ANSARI *et al.* [49] carried out vibration analysis of single-layer graphene sheets using nonlocal elasticity and molecular dynamics. The obtained natural frequencies are matched to derive the appropriate values of the nonlocal parameter. Another way to determine the nonlocal parameter of a certain material is to carry out experimental measurements on vibration behavior. Such measurements for single- and multi-layer graphene resonators are presented respectively by VAN DER ZANDE *et al.* [50] and YUASA *et al.* [51]. Once the separate nonlocal parameters of the FGM constituent phases are determined by following either of these methods, it will be necessary to characterize the spatial variation. This variation depends on the power-law index $n$ defined in Eq. (2.8). The value of $n$ can be adjusted by comparing natural frequencies obtained through the nonlocal analysis to those found by molecular dynamics-based simulations or measured via experimentation.

Displacement field of the nanoplate is expressed in a unified way as

$$u(x, y, z, t) = u_0(x, y, t) - z w_{,x} + f(z)(\varphi_x + w_{,x}), \tag{2.9}$$

$$v(x, y, z, t) = v_0(x, y, t) - z w_{,y} + f(z)(\varphi_y + w_{,y}), \tag{2.10}$$

$$w(x, y, z, t) = w_0(x, y, t), \tag{2.11}$$

where

$$f(z)=\begin{cases}0 & \text{for Kirchhoff plate theory,}\\ z & \text{for Mindlin plate theory,}\\ z\left(1-\dfrac{4z^2}{3h^2}\right) & \text{for third-order shear deformation plate theory.}\end{cases} \tag{2.12}$$

In this representation, $u$, $v$, and $w$ are displacement components in $x$-, $y$-, and $z$-directions, respectively; $u_0$, $v_0$, and $w_0$ are displacements of a point on the midplane $z=0$; $\varphi_x$ and $\varphi_y$ are the rotations of a transverse normal about $y$- and $x$-axes, respectively; and a comma stands for differentiation. Strain field corresponding to these displacements is then found in the form:

$$\varepsilon_{xx}=\frac{1}{2}\left(\frac{\partial u}{\partial x}+\frac{\partial u}{\partial x}\right)=u_{0,x}-zw_{,xx}+f(\varphi_{x,x}+w_{,xx}), \tag{2.13}$$

$$\varepsilon_{yy}=\frac{1}{2}\left(\frac{\partial v}{\partial y}+\frac{\partial v}{\partial y}\right)=v_{0,y}-zw_{,yy}+f(\varphi_{y,y}+w_{,yy}), \tag{2.14}$$

$$\varepsilon_{zz}=\frac{1}{2}\left(\frac{\partial w}{\partial z}+\frac{\partial w}{\partial z}\right)=0, \tag{2.15}$$

$$\begin{aligned}\varepsilon_{xy}&=\frac{1}{2}\left(\frac{\partial u}{\partial y}+\frac{\partial v}{\partial x}\right)\\ &=\frac{1}{2}\{(u_{0,y}+v_{0,x})-2zw_{,xy}+f(\varphi_{x,y}+2w_{,xy}+\varphi_{y,x})\},\end{aligned} \tag{2.16}$$

$$\varepsilon_{yz}=\frac{1}{2}\left(\frac{\partial v}{\partial z}+\frac{\partial w}{\partial y}\right)=\frac{1}{2}f'(\varphi_y+w_{,y}), \tag{2.17}$$

$$\varepsilon_{xz}=\frac{1}{2}\left(\frac{\partial u}{\partial z}+\frac{\partial w}{\partial x}\right)=\frac{1}{2}f'(\varphi_x+w_{,x}. \tag{2.18}$$

For an FGM nanoplate undergoing free vibrations, Hamilton's principle requires that

$$\delta\int_{t_1}^{t_2}(K-U)\,dt=0, \tag{2.19}$$

where $U$ is strain energy and $K$ is kinetic energy. Variations of the energy terms are written as

$$\delta U=\iiint_V(\sigma_{xx}\delta\varepsilon_{xx}+\sigma_{yy}\delta\varepsilon_{yy}+2\sigma_{xy}\delta\varepsilon_{xy}+2\sigma_{xz}\delta\varepsilon_{xz}+2\sigma_{yz}\delta\varepsilon_{yz})\,dV, \tag{2.20}$$

$$\delta K=\iiint_V\rho(z)(\dot{u}\delta\dot{u}+\dot{v}\delta\dot{v}+\dot{w}\delta\dot{w})\,dV. \tag{2.21}$$

Using Eqs. (2.13)–(2.21) and variational principles, the governing partial differential equations are derived as follows:

$$\frac{\partial N_{xx}}{\partial x}+\frac{\partial N_{xy}}{\partial y}=\left\{I_0\frac{\partial^2 u_0}{\partial t^2}-I_1\frac{\partial^3 w}{\partial t^2\partial x}+I_3\left(\frac{\partial^2\varphi_x}{\partial t^2}+\frac{\partial^3 w}{\partial t^2\partial x}\right)\right\} \tag{2.22}$$
$$-\nabla^2\left\{L_0\frac{\partial^2 u_0}{\partial t^2}-L_1\frac{\partial^3 w}{\partial t^2\partial x}+L_3\left(\frac{\partial^2\varphi_x}{\partial t^2}+\frac{\partial^3 w}{\partial t^2\partial x}\right)\right\},$$

$$\frac{\partial N_{yy}}{\partial y}+\frac{\partial N_{xy}}{\partial x}=\left\{I_0\frac{\partial^2 v_0}{\partial t^2}-I_1\frac{\partial^3 w}{\partial t^2\partial y}+I_3\left(\frac{\partial^2\varphi_y}{\partial t^2}+\frac{\partial^3 w}{\partial t^2\partial y}\right)\right\} \tag{2.23}$$
$$-\nabla^2\left\{L_0\frac{\partial^2 v_0}{\partial t^2}-L_1\frac{\partial^3 w}{\partial t^2\partial y}+L_3\left(\frac{\partial^2\varphi_y}{\partial t^2}+\frac{\partial^3 w}{\partial t^2\partial y}\right)\right\},$$

$$\frac{\partial^2 M_{xx}}{\partial x^2}+\frac{\partial^2 M_{yy}}{\partial y^2}+2\frac{\partial^2 M_{xy}}{\partial x\partial y}-\frac{\partial^2 P_{xx}}{\partial x^2}-\frac{\partial^2 P_{yy}}{\partial y^2}-2\frac{\partial^2 P_{xy}}{\partial x\partial y}+\frac{\partial R_{yz}}{\partial y}+\frac{\partial R_{xz}}{\partial x} \tag{2.24}$$
$$=\left\{I_0\frac{\partial^2 w}{\partial t^2}+(I_1-I_3)\left(\frac{\partial^3 u_0}{\partial t^2\partial x}+\frac{\partial^3 v_0}{\partial t^2\partial y}\right)\right.$$
$$\left.+(-I_2+2I_4-I_5)\left(\frac{\partial^4 w}{\partial t^2\partial x^2}+\frac{\partial^4 w}{\partial t^2\partial y^2}\right)+(I_4-I_5)\left(\frac{\partial^3\varphi_x}{\partial t^2\partial x}+\frac{\partial^3\varphi_y}{\partial t^2\partial y}\right)\right\}$$
$$-\nabla^2\left\{L_0\frac{\partial^2 w}{\partial t^2}+(L_1-L_3)\left(\frac{\partial^3 u_0}{\partial t^2\partial x}+\frac{\partial^3 v_0}{\partial t^2\partial y}\right)\right.$$
$$\left.+(-L_2+2L_4-L_5)\left(\frac{\partial^4 w}{\partial t^2\partial x^2}+\frac{\partial^4 w}{\partial t^2\partial y^2}\right)+(L_4-L_5)\left(\frac{\partial^3\varphi_x}{\partial t^2\partial x}+\frac{\partial^3\varphi_y}{\partial t^2\partial y}\right)\right\},$$

$$\frac{\partial P_{xx}}{\partial x}+\frac{\partial P_{xy}}{\partial y}-R_{xz}=\left\{I_3\frac{\partial^2 u_0}{\partial t^2}-I_4\frac{\partial^3 w}{\partial t^2\partial x}+I_5\left(\frac{\partial^2\varphi_x}{\partial t^2}+\frac{\partial^3 w}{\partial t^2\partial x}\right)\right\} \tag{2.25}$$
$$-\nabla^2\left\{L_3\frac{\partial^2 u_0}{\partial t^2}-L_4\frac{\partial^3 w}{\partial t^2\partial x}+L_5\left(\frac{\partial^2\varphi_x}{\partial t^2}+\frac{\partial^3 w}{\partial t^2\partial x}\right)\right\},$$

$$\frac{\partial P_{yy}}{\partial y}+\frac{\partial P_{xy}}{\partial x}-R_{yz}=\left\{I_3\frac{\partial^2 v_0}{\partial t^2}-I_4\frac{\partial^3 w}{\partial t^2\partial y}+I_5\left(\frac{\partial^2\varphi_y}{\partial t^2}+\frac{\partial^3 w}{\partial t^2\partial y}\right)\right\} \tag{2.26}$$
$$-\nabla^2\left\{L_3\frac{\partial^2 v_0}{\partial t^2}-L_4\frac{\partial^3 w}{\partial t^2\partial y}+L_5\left(\frac{\partial^2\varphi_y}{\partial t^2}+\frac{\partial^3 w}{\partial t^2\partial y}\right)\right\}.$$

The boundary conditions are obtained as

$$u_0=0, \quad \text{or} \quad N_{xx}n_x+N_{xy}n_y=0, \tag{2.27}$$

$$v_0=0, \quad \text{or} \quad N_{xy}n_x+N_{yy}n_y=0, \tag{2.28}$$

$$\varphi_x=0, \quad \text{or} \quad P_{xx}n_x+P_{xy}n_y=0, \tag{2.29}$$

$$\varphi_y=0, \quad \text{or} \quad P_{xy}n_x+P_{yy}n_y=0, \tag{2.30}$$

$$w=0, \quad \text{or} \tag{2.31}$$

$$\left(\frac{\partial M_{xx}}{\partial x}+\frac{\partial M_{xy}}{\partial y}-\frac{\partial P_{xx}}{\partial x}-\frac{\partial P_{xy}}{\partial y}+R_{xz}\right)n_x + \left(\frac{\partial M_{yy}}{\partial y}+\frac{\partial M_{xy}}{\partial x}-\frac{\partial P_{yy}}{\partial y}-\frac{\partial P_{xy}}{\partial x}+R_{yz}\right)n_y$$
$$= (I_1-I_3)\left(\frac{\partial^2 u_0}{\partial t^2}n_x+\frac{\partial^2 v_0}{\partial t^2}n_y\right)+(-I_2+2I_4-I_5)\left(\frac{\partial^3 w}{\partial x\partial t^2}n_x+\frac{\partial^3 w}{\partial y\partial t^2}n_y\right)$$
$$+(I_4-I_5)\left(\frac{\partial^2 \varphi_x}{\partial t^2}n_x+\frac{\partial^2 \varphi_y}{\partial t^2}n_y\right)-\nabla^2\left\{(L_1-L_3)\left(\frac{\partial^2 u_0}{\partial t^2}n_x+\frac{\partial^2 v_0}{\partial t^2}n_y\right)\right.$$
$$\left.+(-L_2+2L_4-L_5)\left(\frac{\partial^3 w}{\partial x\partial t^2}n_x+\frac{\partial^3 w}{\partial y\partial t^2}n_y\right)+(L_4-L_5)\left(\frac{\partial^2 \varphi_x}{\partial t^2}n_x+\frac{\partial^2 \varphi_y}{\partial t^2}n_y\right)\right\},$$

$$\frac{\partial w}{\partial x}=0, \qquad \text{or} \qquad (M_{xx}-P_{xx})n_x+(M_{xy}-P_{xy})n_y=0, \tag{2.32}$$

$$\frac{\partial w}{\partial y}=0, \qquad \text{or} \qquad (M_{xy}-P_{xy})n_x+(M_{yy}-P_{yy})n_y=0, \tag{2.33}$$

where $n_x$ and $n_y$ are the components of the unit outward normal vector.

Stress resultants and coefficient terms in the governing equations and boundary conditions are defined by

$$\begin{Bmatrix} N_{\alpha\beta} \\ M_{\alpha\beta} \\ P_{\alpha\beta} \end{Bmatrix} = \int_{-h/2}^{h/2} (1-\mu(z)\nabla^2)\sigma_{\alpha\beta} \begin{Bmatrix} 1 \\ z \\ f \end{Bmatrix} dz,$$
$$\begin{Bmatrix} N_{\alpha z} \\ R_{\alpha z} \end{Bmatrix} = \int_{-h/2}^{h/2} (1-\mu(z)\nabla^2)\sigma_{\alpha z} \begin{Bmatrix} 1 \\ f' \end{Bmatrix} dz, \quad \alpha,\beta = x,y, \tag{2.34}$$

$$\begin{Bmatrix} I_0 \\ I_1 \\ I_2 \\ I_3 \\ I_4 \\ I_5 \end{Bmatrix} = \int_{-h/2}^{h/2} \rho(z) \begin{Bmatrix} 1 \\ z \\ z^2 \\ f \\ zf \\ f^2 \end{Bmatrix} dz, \quad \begin{Bmatrix} L_0 \\ L_1 \\ L_2 \\ L_3 \\ L_4 \\ L_5 \end{Bmatrix} = \int_{-h/2}^{h/2} \mu(z)\rho(z) \begin{Bmatrix} 1 \\ z \\ z^2 \\ f \\ zf \\ f^2 \end{Bmatrix} dz. \tag{2.35}$$

## 3. Numerical solution

The generalized differential quadrature method (GDQM) [52] is used to solve the equation system comprising governing partial differential equations and boundary conditions. In the GDQM, $n$th derivative of a function $f$ is expressed

as follows:

$$\frac{\partial^n f(x,t)}{\partial x^n}|_{x=x_i} = \sum_{j=1}^{N} c_{ij}^{(n)} f(x_j,t), \qquad i = 1,\dots,N, \tag{3.1}$$

where $c_{ij}^{(n)}$ are weighting coefficients [53] for the $n$th-order derivative and $N$ is the number of nodes. In parametric analyses, we consider two different types of nanoplate configurations: a nanoplate simply-supported on all edges and a cantilever nanoplate fixed at $x = 0$. For both simply-supported and cantilever nanoplates, nodal points are identified as Chebyshev–Gauss–Lobatto points, which are given by

$$x_i = \frac{1}{2}\left\{1 - \cos\left(\frac{\pi(i-1)}{N-1}\right)\right\}, \qquad i = 1,\dots,N. \tag{3.2}$$

Series forms of the governing equations are derived by applying the representation in Eq. (3.1). These equations are provided in the Appendix.

For a simply-supported nanoplate, series forms of boundary conditions at $y = 0$ and $y = b$ read:

$$u_0 = v_0 = w = \varphi_x = 0, \tag{3.3}$$

$$A_3 \sum_{k=1}^{N_y} c_{jk}^{(1)} v_{0_{i,k}} + (A_5 - A_4) \sum_{k=1}^{N_y} c_{jk}^{(2)} w_{i,k} + A_5 \sum_{k=1}^{N_y} c_{jk}^{(1)} \varphi_{y_{i,k}} = 0, \tag{3.4}$$

$$A_1 \sum_{k=1}^{N_y} c_{jk}^{(1)} v_{0_{i,k}} + (A_4 - A_2) \sum_{k=1}^{N_y} c_{jk}^{(2)} w_{i,k} + A_4 \sum_{k=1}^{N_y} c_{jk}^{(1)} \varphi_{y_{i,k}} = 0, \tag{3.5}$$

and at $x = 0$, $x = a$, we have

$$u_0 = v_0 = w = \varphi_y = 0, \tag{3.6}$$

$$A_3 \sum_{k=1}^{N_x} c_{ik}^{(1)} u_{0_{k,j}} + (A_5 - A_4) \sum_{k=1}^{N_x} c_{ik}^{(2)} w_{k,j} + A_5 \sum_{k=1}^{N_x} c_{ik}^{(1)} \varphi_{x_{k,j}} = 0, \tag{3.7}$$

$$A_1 \sum_{k=1}^{N_x} c_{ik}^{(1)} u_{0_{k,j}} + (A_4 - A_2) \sum_{k=1}^{N_x} c_{ik}^{(2)} w_{k,j} + A_4 \sum_{k=1}^{N_x} c_{ik}^{(1)} \varphi_{x_{k,j}} = 0. \tag{3.8}$$

The coefficients in the governing equations and boundary conditions are given by:

$$
\begin{Bmatrix} A_0 \\ A_1 \\ A_2 \\ A_3 \\ A_4 \\ A_5 \end{Bmatrix} = \int_{-h/2}^{h/2} Q_{11} \begin{Bmatrix} 1 \\ z \\ z^2 \\ f(z) \\ zf(z) \\ (f(z))^2 \end{Bmatrix} dz, \quad \begin{Bmatrix} B_0 \\ B_1 \\ B_2 \\ B_3 \\ B_4 \\ B_5 \end{Bmatrix} = \int_{-h/2}^{h/2} Q_{12} \begin{Bmatrix} 1 \\ z \\ z^2 \\ f(z) \\ zf(z) \\ (f(z))^2 \end{Bmatrix} dz,
$$

$$
\begin{Bmatrix} C_0 \\ C_1 \\ C_2 \\ C_3 \\ C_4 \\ C_5 \\ C_6 \end{Bmatrix} = \int_{-h/2}^{h/2} Q_{66} \begin{Bmatrix} 1 \\ z \\ z^2 \\ f(z) \\ zf(z) \\ (f(z))^2 \\ (f'(z))^2 \end{Bmatrix} dz. \tag{3.9}
$$

Series forms of the boundary conditions for the cantilever nanoplate are derived in a similar manner, and not provided here for brevity.

For both simply-supported and cantilever nanoplates, governing equations and boundary conditions are consolidated into the following matrix form:

$$
(\mathbf{K} - \Omega^2 \mathbf{M}) d^* = 0, \tag{3.10}
$$

where $\Omega$ is natural frequency, $\mathbf{K}$ is stiffness matrix, $\mathbf{M}$ is mass matrix and $\mathbf{d}^*$ is mode shape vector expressed as

$$
d^* = \{\{u_i^*\}^T, \{v_i^*\}^T, \{w_i^*\}^T, \{\varphi_{x_i}^*\}^T, \{\varphi_{y_i}^*\}^T\}^T, \quad i = 1, \ldots, N_x \times N_y. \tag{3.11}
$$

## 4. Numerical results

In parametric analyses, we examine free vibrations of ceramic-metal functionally graded nano-plates, whose constituents are silicon nitride ($Si_3N_4$) and stainless steel. Properties for this material pair are given by

$$
E_c = 348.43 \text{ GPa}, \quad \nu_c = 0.3, \quad \rho_c = 2370 \text{ kg/m}^3, \tag{4.1}
$$

$$
E_m = 201.04 \text{ GPa}, \quad \nu_m = 0.3, \quad \rho_m = 8166 \text{ kg/m}^3. \tag{4.2}
$$

The nonlocal parameter of the metallic phase is taken as $\mu_m = 2$ nm$^2$, which is a reference value adopted in various studies in the literature [26, 28]. The degree of variation in the nonlocal parameter is quantified by the ratio $\mu_c/\mu_m$. When the nonlocal parameter is assumed to be constant $\mu_c/\mu_m$ is equal to unity, whereas when $\mu$ varies across the thickness $\mu_c/\mu_m \neq 1$. We set $\mu_c/\mu_m$ as 2 in a number of parametric analyses. In remaining cases, it is varied so as to assess the influence of the nonlocal parameter variation.

To be able to verify theoretical and computational developments, in Table 1 we provide comparisons to the results given by ZARE *et al.* [25]. The article by ZARE *et al.* [25] presents solutions regarding free vibrations of functionally graded rectangular nanoplates developed under the assumption of constant nonlocal parameter. Material properties used in [25] are the same as those given by Eqs. (4.1) and (4.2). The table tabulates first three dimensionless natural frequencies of a simply-supported functionally graded nanoplate. Dimensionless natural frequency is defined as

$$\omega = \Omega h \sqrt{\frac{2(1+\nu_c)\rho_c}{E_c}}. \tag{4.3}$$

**Table 1. Comparisons of dimensionless first three natural frequencies calculated for a simply-supported functionally graded nanoplate possessing a constant nonlocal parameter $\mu$: $n = 5$, $a = 10$ nm, $a/h = 20$.**

| $a/b$ | $\mu_c = \mu_m = \mu$ (in nm$^2$) | | $\omega_1$ | $\omega_2$ | $\omega_3$ |
|---|---|---|---|---|---|
| 1 | 0 | Present study | 0.0114 | 0.0285 | 0.0285 |
| | | ZARE *et al.* [25] | 0.0114 | 0.0281 | 0.0281 |
| | 1 | Present study | 0.0104 | 0.0233 | 0.0233 |
| | | ZARE *et al.* [25] | 0.0104 | 0.0230 | 0.0230 |
| | 4 | Present study | 0.0085 | 0.0165 | 0.0165 |
| | | ZARE *et al.* [25] | 0.0085 | 0.0165 | 0.0165 |
| 2 | 0 | Present study | 0.0285 | 0.0454 | 0.0732 |
| | | ZARE *et al.* [25] | 0.0281 | 0.0443 | 0.0704 |
| | 1 | Present study | 0.0233 | 0.0340 | 0.0484 |
| | | ZARE *et al.* [25] | 0.0230 | 0.0330 | 0.0466 |
| | 4 | Present study | 0.0165 | 0.0223 | 0.0296 |
| | | ZARE *et al.* [25] | 0.0165 | 0.0218 | 0.0286 |

Both our results and those given in [25] are generated by using Kirchhoff plate theory. The excellent agreement between the natural frequencies is indicative of the high degree of accuracy achieved by the application of the proposed procedures.

In Figs. 2–10 and Tables 2 and 3, we provide parametric analyses for functionally graded rectangular nanoplates possessing a spatially variable nonlocal parameter. Figure 2 depicts dimensionless first natural frequencies of simply-supported and cantilever nanoplates as a function of the dimensionless plate length $a/\sqrt{\mu_m}$. All three plate theories, i.e., the Kirchhoff plate theory (KPT), the Mindlin plate theory (MPT), and the third-order shear deformation theory

(TSDT) are considered. For both simply-supported and cantilever nanoplates, $\omega_1$ increases with a corresponding increase in $a/\sqrt{\mu_m}$; and levels off around a constant attained at larger values of dimensionless plate length. The constants are the vibration frequencies of a classical macroscale plate, for which numerical results can be found by setting $\mu_c = \mu_m = 0$. Hence, as expected, size effect turns out to be important, especially for relatively smaller values of the ratio $a/\sqrt{\mu_m}$. Curves generated by the KPT and MPT enclose that computed by using the TSDT. The differences in Fig. 2b seem to be larger compared to those found in Fig. 2a. However, when percent differences are evaluated by setting the KPT as the reference, it can be seen that the percent differences calculated in Fig. 2a are greater. The larger percent difference found in the simply-supported plate is primarily due to a higher degree of constraint. Three of the edges of the cantilever plate are free, and all-around constraints for the simply-supported plate lead to a larger shear effect. This causes a more significant difference between the predictions of the plate theories. Let us note that in the KPT the transverse shear strain is assumed to be zero, whereas in the Mindlin theory the transverse shear is constant across the thickness. The TSDT presumes parabolic variation of transverse shear strain. Larger differences are expected in cases where shear deformations are more pronounced.

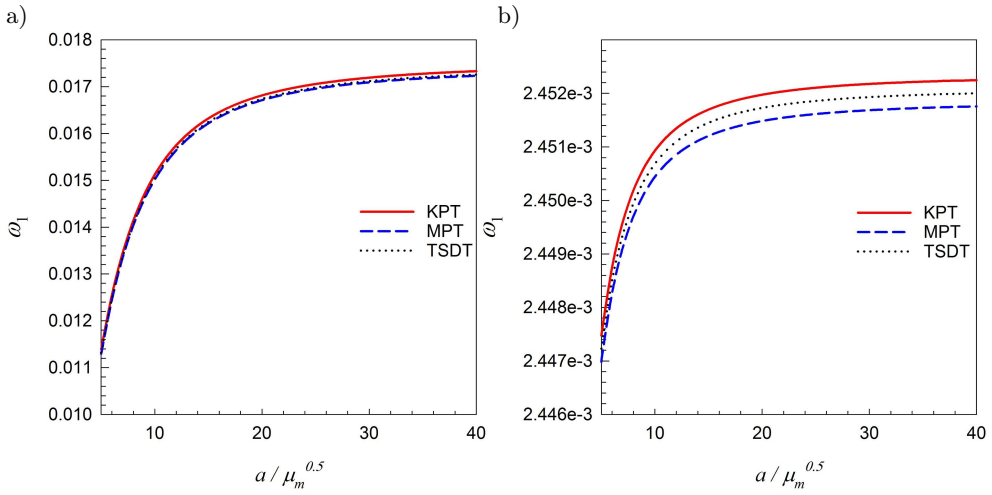


Fig. 2. Dimensionless first natural frequency $\omega_1$ vs. $a/\sqrt{\mu_m}$ for three different plate theories: a) simply-supported nanoplate, b) cantilever nanoplate. $a/b = 4/3$, $ah = 20$, $\mu_m = 2$ nm$^2$, $\mu_c/\mu_m = 2$, $n = 2$.

The numerical results given in Fig. 3 regarding second natural frequency point out to similar trends, except for more pronounced differences among the results obtained for different plate theories. It can be seen that differences be-

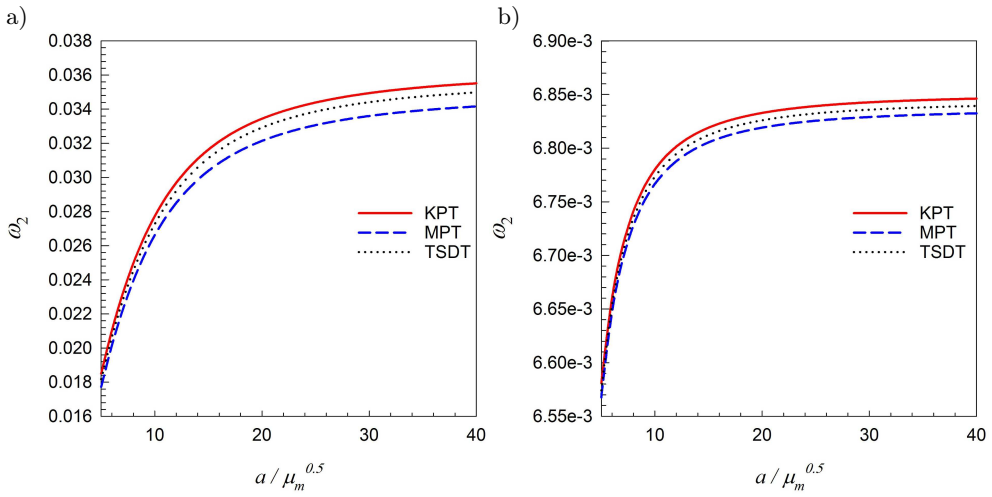


FIG. 3. Dimensionless second natural frequency $\omega_2$ vs. $a/\sqrt{\mu_m}$ for three different plate theories: a) simply-supported nanoplate, b) cantilever nanoplate. $a/b = 4/3$, $a/h = 20$, $\mu_m = 2$ nm$^2$, $\mu_c/\mu_m = 2$, $n = 2$.

tween the predictions of plate theories get larger as mode number increases. This observation is also related to main assumptions on through-the-thickness transverse shear distribution. Shear effect is more prominent in higher modes, and causes larger differences between the results obtained for different plate theories. Mathematical proof demonstrating larger difference in higher modes is provided by WANG *et al.* [54]. With its quadratic transverse shear strain distribution, the TSDT is expected to produce results within a higher degree of accuracy.

The first two mode shapes of simply-supported and cantilever nanoplates for $a/\sqrt{\mu_m} = 10$ are provided in Fig. 4. The TSDT is used in the generation of the mode shapes and the remaining sets of results presented in this section. Figures 5 and 6 depict the influence of the nonlocal parameter ratio $\mu_c/\mu_m$ on respectively $\omega_1$ and $\omega_2$. For both simply-supported and cantilever nanoplates, nonlocal parameter ratio has a significant impact on the dimensionless natural frequency. This finding implies that variation of the nonlocal parameter needs to be taken into account to be able to produce more realistic numerical results. Both of the dimensionless natural frequencies $\omega_1$ and $\omega_2$ get smaller as the ratio $\mu_c/\mu_m$ is increased from 0.5 to 4.0. Notice that natural frequencies merge at a single value as the dimensionless plate length $a/\sqrt{\mu_m}$ gets larger. This single value is again the frequency obtained for a classical plate by taking $\mu_c = \mu_m = 0$.

Further results regarding the influence of $\mu_c/\mu_m$ on dimensionless frequencies $\omega_1$ and $\omega_2$ are given in Tables 2 and 3. Dependence on $\mu_c/\mu_m$ is examined by considering different values of dimensionless plate length $a/\sqrt{\mu_m}$ and aspect

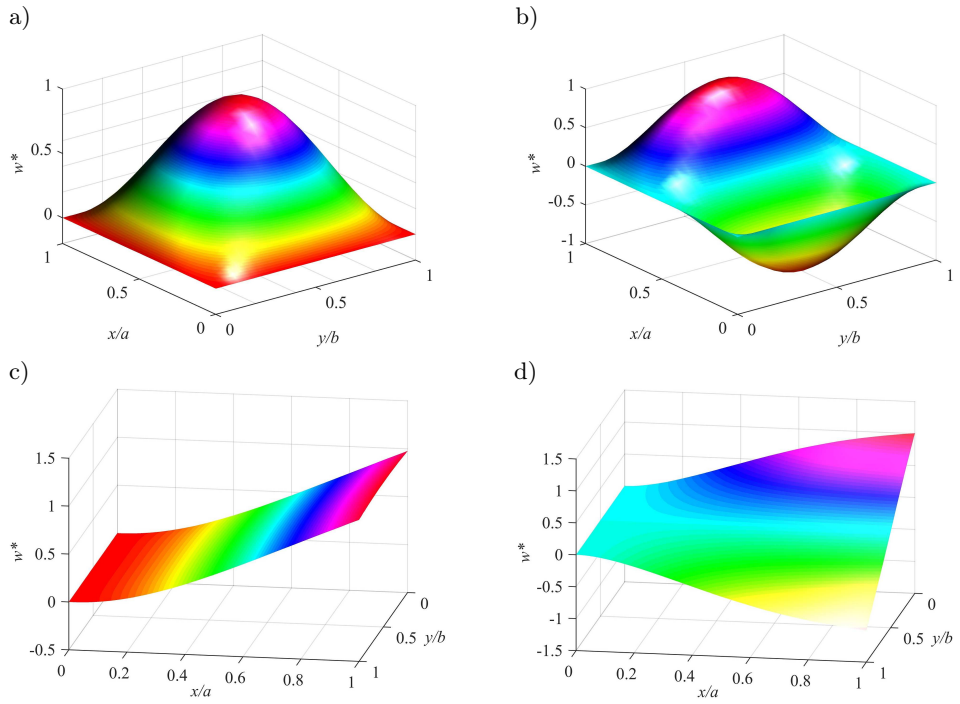


FIG. 4. First two mode shapes of simply-supported and cantilever nanoplates: a) first mode shape of simply supported nanoplate, $\omega_1 = 0.015$, b) second mode-shape of simply-supported nanoplate, $\omega_2 = 0.027$, c) first mode shape of cantilever nanoplate, $\omega_1 = 2.451 \times 10^{-3}$, d) second mode shape of cantilever nanoplate, $\omega_2 = 6.774 \times 10^{-3}$, $a/\sqrt{\mu_m} = 10$, $a/b = 4/3$, $a/h = 20$, $\mu_m = 2$ nm$^2$, $\mu_c/\mu_m = 2$, $n = 2$.

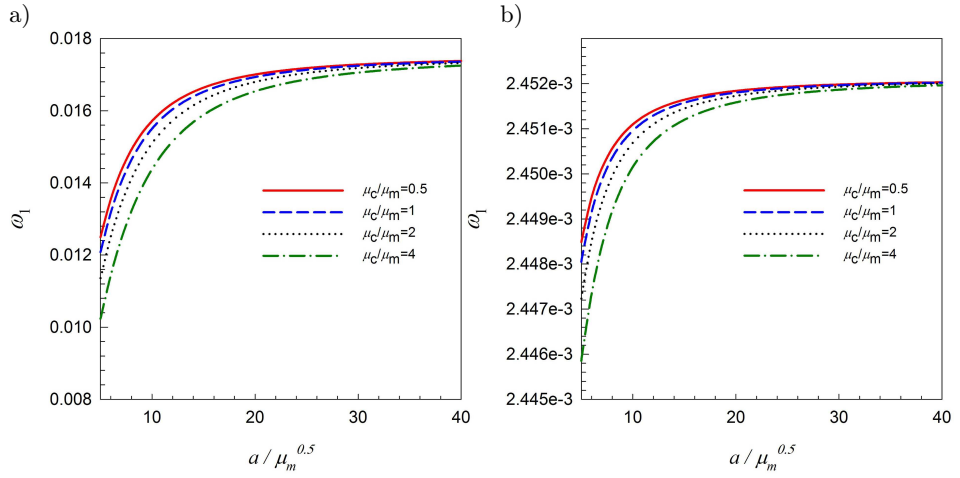


FIG. 5. Dimensionless first natural frequency $\omega_1$ vs. $a/\sqrt{\mu_m}$ for different values of $\mu_c/\mu_m$: a) simply-supported nanoplate, b) cantilever nanoplate, $a/b = 4/3$, $a/h = 20$, $n = 2$, $\mu_m = 2$ nm$^2$.

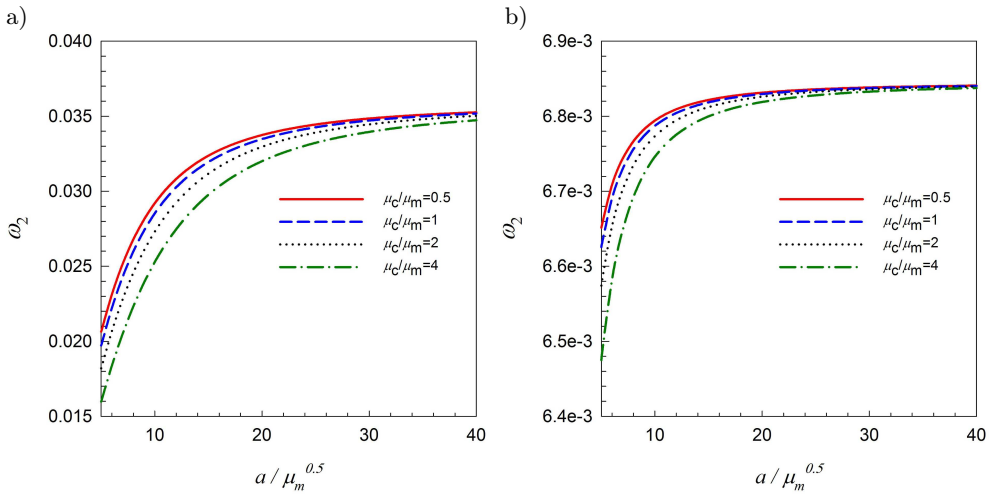


FIG. 6. Dimensionless second natural frequency $\omega_2$ vs. $a/\sqrt{\mu_m}$ for different values of $\mu_c/\mu_m$: a) simply-supported nanoplate, b) cantilever nanoplate, $a/b = 4/3$, $a/h = 20$, $n = 2$, $\mu_m = 2$ nm$^2$.

ratio $a/b$. In all cases, dimensionless frequencies are decreasing functions of the nonlocal parameter ratio $\mu_c/\mu_m$. However, an increase in the aspect ratio $a/b$ causes an increase in the dimensionless natural frequencies.

In Figs. 7 and 8, we present $\omega_1$ and $\omega_2$ as functions of the power-law index $n$ and dimensionless plate length $a/\sqrt{\mu_m}$. In order to present the influence of the dimensionless plate length more clearly, the results pertaining to the cantilever plate are provided in two separate figures (Figs. 7b, c and 8b, c), which include horizontal drop lines. The index $n$ controls the variation of the ceramic

**Table 2. Dimensionless first natural frequencies of simply-supported and cantilever nanoplates: $a/h = 20$, $n = 2$, $\mu_m = 2$ nm$^2$.**

| | | Simply-supported nanoplate | | Cantilever nanoplate | |
|---|---|---|---|---|---|
| | | $a/\sqrt{\mu_m} = 5$ | $a/\sqrt{\mu_m} = 10$ | $a/\sqrt{\mu_m} = 5$ | $a/\sqrt{\mu_m} = 10$ |
| $\frac{a}{b} = \frac{1}{2}$ | $\mu_c/\mu_m = 0.5$ | 6.6127e-3 | 7.5184e-3 | 1.9457e-3 | 1.9575e-3 |
| | $\mu_c/\mu_m = 1$ | 6.4742e-3 | 7.4665e-3 | 1.9454e-3 | 1.9574e-3 |
| | $\mu_c/\mu_m = 2$ | 6.2215e-3 | 7.3657e-3 | 1.9450e-3 | 1.9573e-3 |
| | $\mu_c/\mu_m = 4$ | 5.7938e-3 | 7.1757e-3 | 1.9444e-3 | 1.9570e-3 |
| $\frac{a}{b} = 1$ | $\mu_c/\mu_m = 0.5$ | 9.7128e-3 | 1.1667e-2 | 2.2529e-3 | 2.2547e-3 |
| | $\mu_c/\mu_m = 1$ | 9.4402e-3 | 1.1545e-2 | 2.2526e-3 | 2.2546e-3 |
| | $\mu_c/\mu_m = 2$ | 8.9575e-3 | 1.1314e-2 | 2.2522e-3 | 2.2545e-3 |
| | $\mu_c/\mu_m = 4$ | 8.1795e-3 | 1.0889e-2 | 2.2514e-3 | 2.2541e-3 |

**Table 3. Dimensionless second natural frequencies of simply-supported and cantilever nanoplates: $a/h = 20$, $n = 2$, $\mu_m = 2$ nm$^2$.**

| | | Simply-supported nanoplate | | Cantilever nanoplate | |
|---|---|---|---|---|---|
| | | $a/\sqrt{\mu_m} = 5$ | $a/\sqrt{\mu_m} = 10$ | $a/\sqrt{\mu_m} = 5$ | $a/\sqrt{\mu_m} = 10$ |
| $\frac{a}{b} = \frac{1}{2}$ | $\mu_c/\mu_m = 0.5$ | 9.6723e-3 | 1.1618e-2 | 3.2856e-3 | 3.3026e-3 |
| | $\mu_c/\mu_m = 1$ | 9.4009e-3 | 1.1497e-2 | 3.2825e-3 | 3.3018e-3 |
| | $\mu_c/\mu_m = 2$ | 8.9204e-3 | 1.1267e-2 | 3.2764e-3 | 3.3001e-3 |
| | $\mu_c/\mu_m = 4$ | 8.1457e-3 | 1.0844e-2 | 3.2649e-3 | 3.2968e-3 |
| $\frac{a}{b} = 1$ | $\mu_c/\mu_m = 0.5$ | 1.8760e-2 | 2.5917e-2 | 5.3673e-3 | 5.4606e-3 |
| | $\mu_c/\mu_m = 1$ | 1.7963e-2 | 2.5374e-2 | 5.3502e-3 | 5.4561e-3 |
| | $\mu_c/\mu_m = 2$ | 1.6634e-2 | 2.4383e-2 | 5.3165e-3 | 5.4471e-3 |
| | $\mu_c/\mu_m = 4$ | 1.4673e-2 | 2.2706e-2 | 5.2510e-3 | 5.4291e-3 |

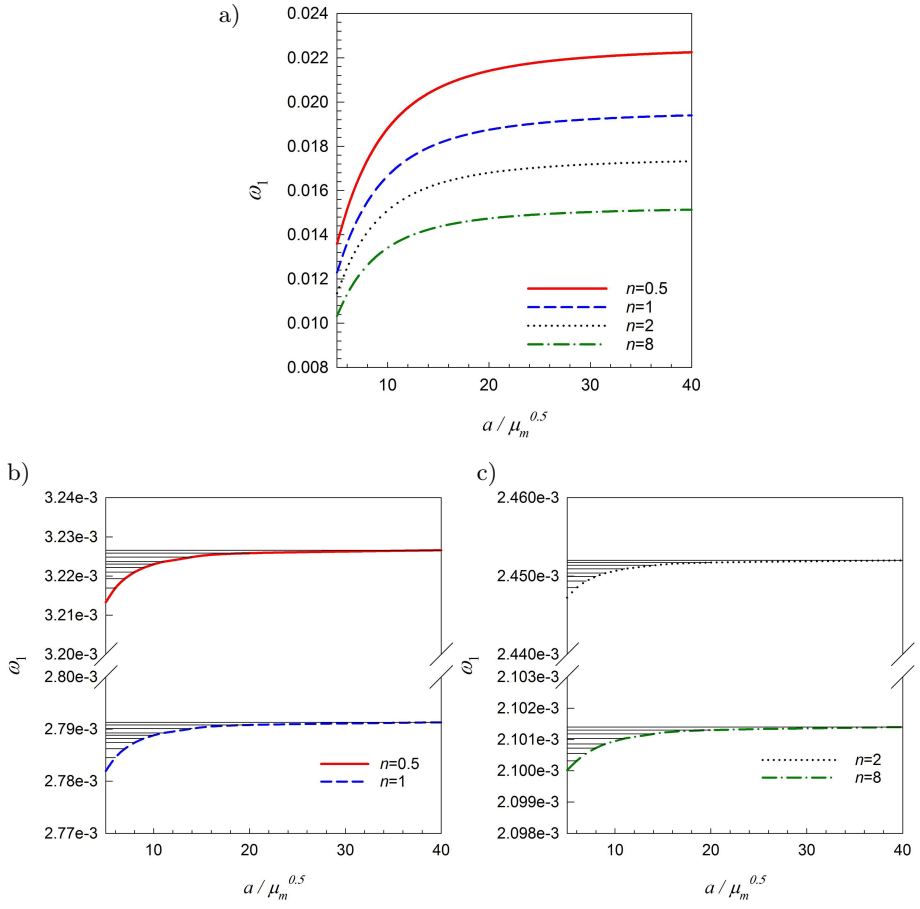


FIG. 7. Dimensionless first natural frequency $\omega_1$ vs. $a/\sqrt{\mu_m}$ for various values of the power-law index $n$: a) simply-supported nanoplate, b) cantilever nanoplate, $n = 0.5, 1$, c) cantilever nano-plate $n = 2, 8$, $a/b = 4/3$, $a/h = 20$, $\mu_m = 2$ nm$^2$, $\mu_c/\mu_m = 2$.

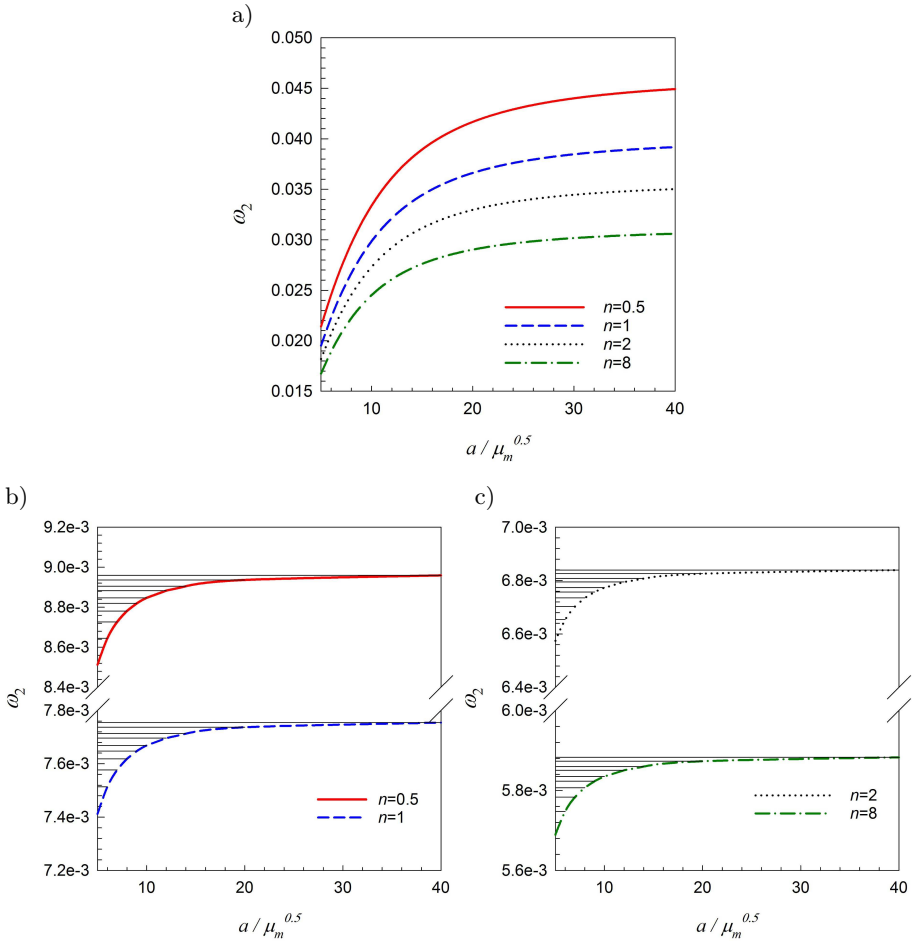


FIG. 8. Dimensionless second natural frequency $\omega_2$ vs. $a/\sqrt{\mu_m}$ for various values of the power-law index $n$: a) simply-supported nanoplate, b) cantilever nanoplate, $n = 0.5, 1$, c) cantilever nanoplate, $n = 2, 8$, $a/b = 4/3$, $a/h = 20$, $\mu_m = 2$ nm$^2$, $\mu_c/\mu_m = 2$.

volume fraction as indicated by Eq. (2.8). The nanoplate is ceramic-rich if $n < 1$, and metal-rich if $n > 1$. Both of the dimensionless natural frequencies $\omega_1$ and $\omega_2$ decrease as the exponent $n$ is increased from 0.5 to 8. Thus, ceramic-rich functionally graded nano-plates possess larger natural frequencies. This is the expected result since the ceramic phase of the FGM composite nanoplate has larger elastic modulus and lower density compared to the metallic phase. The constants attained for larger $a/\sqrt{\mu_m}$ are equal to the frequencies predicted by the classical plate theory.

Parametric analysis regarding the effects of the power-law index $n$ and the nonlocal parameter ratio $\mu_c/\mu_m$ on the first four dimensionless natural frequen-

cies of a simply-supported FGM nano-plate are presented in Figs. 9 and 10. These figures clearly show how the natural frequencies increase as the power-law index $n$ gets smaller. Ceramic-rich functionally graded composite nanoplates are again shown to possess significantly larger natural frequencies than the metal-rich nanoplates. The nonlocal parameter ratio $\mu_c/\mu_m$ also imparts a notable influence on all four natural frequencies. Sensitivity of the frequencies to the

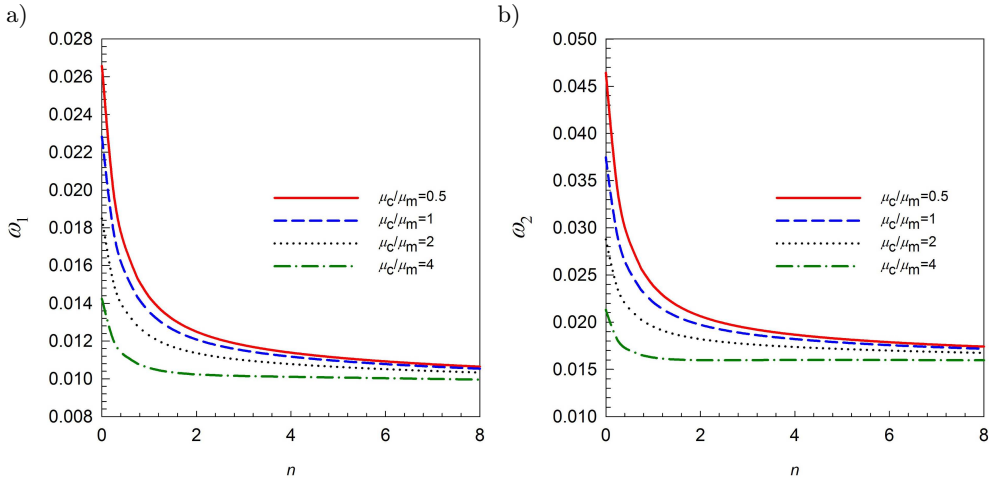


FIG. 9. Dimensionless natural frequencies of a simply-supported nanoplate as functions of $n$ and $\mu_c/\mu_m$: a) first natural frequency $\omega_1$, b) second natural frequency $\omega_2$, $a/\sqrt{\mu_m} = 5$, $a//b = 4/3$, $a/h = 20$, $\mu_m = 2$ nm$^2$.

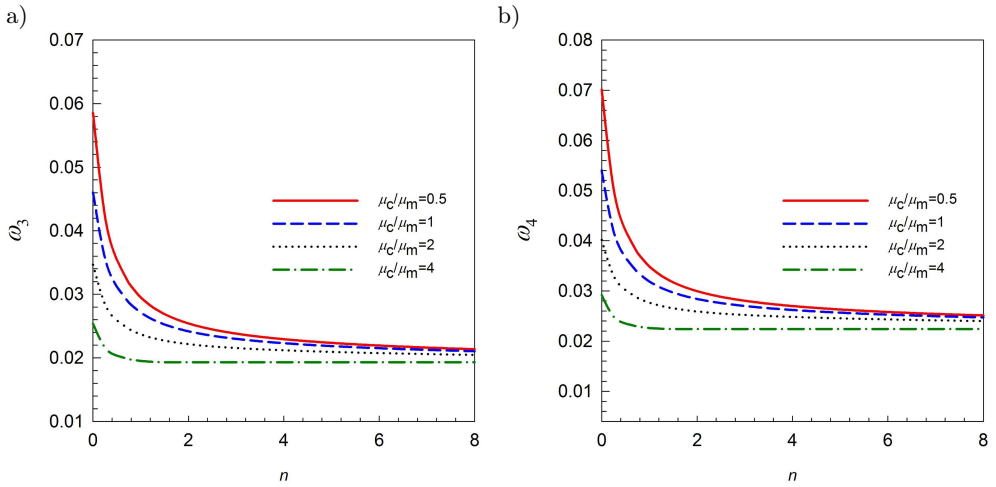


FIG. 10. Dimensionless natural frequencies of a simply-supported nanoplate as functions of $n$ and $\mu_c/\mu_m$: a) third natural frequency $\omega_3$, b) fourth natural frequency $\omega_4$, $a/\sqrt{\mu_m} = 5$, $a//b = 4/3$, $a/h = 20$, $\mu_m = 2$ nm$^2$.

change in the nonlocal parameter ratio points to the fact that the nonlocal parameter variation should be accounted for in dynamic analysis, which is the basic hypothesis of the present study.

## 5. Concluding remarks

In this article, we outline a nonlocal elasticity-based method for free vibration analysis of functionally graded rectangular nanoplates. The method developed is capable of accounting for the spatial variation of the nonlocal parameter. Governing equations and boundary conditions are derived by following the variational approach and applying Hamilton's principle. All material properties, including the nonlocal parameter, are assumed to be functions of the thickness coordinate in the derivations. Displacement field is expressed in a unified way in the formulation to be able to generate results for three plate theories. The derived equations are solved numerically by means of generalized differential quadrature method. Proposed procedure is verified through comparisons made with the results available in the literature. Further numerical results are provided to demonstrate the effects of dimensionless plate length, nonlocal parameter ratio, and power-law index on the natural vibration frequencies of simply-supported and cantilever nanoplates.

Vibration frequencies calculated for the three different plate theories show that the KPT predicts higher natural frequencies and stiffer nanoplate behavior. The results obtained for the TSDT lie in between those calculated for the Kirchhoff and Mindlin plate theories. In all cases, as the dimensionless plate length $a/\sqrt{\mu_m}$ is increased, vibration frequencies first increase and then approach constant values. For a given configuration, the constant attained at large $a/\sqrt{\mu_m}$ is equal to the frequency computed for a plate whose nonlocal parameter $\mu$ is zero. In other words, the results corresponding to macro-scale plates are recovered for larger $a/\sqrt{\mu_m}$, which points out to the size effect's dominance for smaller plate length. The influence of the nonlocal parameter ratio $\mu_c/\mu_m$ is shown to be important. Increase in $\mu_c/\mu_m$ causes drops in the dimensionless natural frequencies. This finding implies that assuming a constant nonlocal parameter might lead to results of reduced accuracy. Thus, reliable results regarding free vibrations of functionally graded rectangular nanoplates can be produced by taking into account the nonlocal parameter variation. The methods presented in this article could prove to be useful in this respect and in analysis, design, and optimization of graded composite nanoplate structures.

## Acknowledgement

This work was supported by the Scientific and Technological Research Council of Turkey (TÜBİTAK) through grant 213M606.

## Appendix

Series forms of the governing equations are derived as follows:

$$
\begin{aligned}
\text{(A1)}\quad & A_0\sum_{k=1}^{N_x} c_{ik}^{(2)} u_{0_{k,j}} + C_0\sum_{k=1}^{N_y} c_{jk}^{(2)} u_{0_{i,k}} + (B_0+C_0)\sum_{m=1}^{N_y} c_{jm}^{(1)}\sum_{k=1}^{N_x} c_{ik}^{(1)} v_{0_{k,m}} \\
& + (A_3-A_1)\sum_{k=1}^{N_x} c_{ik}^{(3)} w_{k,j} + (B_3-B_1-2C_1+2C_3)\sum_{m=1}^{N_y} c_{jm}^{(2)}\sum_{k=1}^{N_x} c_{ik}^{(1)} w_{k,m} \\
& + A_3\sum_{k=1}^{N_x} c_{ik}^{(2)}\varphi_{x_{k,j}} + C_3\sum_{k=1}^{N_y} c_{jk}^{(2)}\varphi_{x_{i,k}} + (B_3+C_3)\sum_{m=1}^{N_y} c_{jm}^{(1)}\sum_{k=1}^{N_x} c_{ik}^{(1)}\varphi_{y_{k,m}} \\
= {} & I_0\ddot{u}_0 + (I_3-I_1)\sum_{k=1}^{N_x} c_{ik}^{(1)}\ddot{w}_{k,j} + I_3\ddot{\varphi}_x - L_0\sum_{k=1}^{N_x} c_{ik}^{(2)}\ddot{u}_{0_{k,j}} \\
& - (L_3-L_1)\sum_{k=1}^{N_x} c_{ik}^{(3)}\ddot{w}_{k,j} - L_3\sum_{k=1}^{N_x} c_{ik}^{(2)}\ddot{\varphi}_{x_{k,j}} - L_0\sum_{k=1}^{N_y} c_{jk}^{(2)}\ddot{u}_{0_{i,k}} \\
& - (L_3-L_1)\sum_{m=1}^{N_y} c_{jm}^{(2)}\sum_{k=1}^{N_x} c_{ik}^{(1)}\ddot{w}_{k,m} - L_3\sum_{k=1}^{N_y} c_{jk}^{(2)}\ddot{\varphi}_{x_{i,k}},
\end{aligned}
$$

$$
\begin{aligned}
\text{(A2)}\quad & C_0\sum_{k=1}^{N_x} c_{ik}^{(2)} v_{0_{k,j}} + A_0\sum_{k=1}^{N_y} c_{jk}^{(2)} v_{0_{i,k}} + (B_0+C_0)\sum_{m=1}^{N_y} c_{jm}^{(1)}\sum_{k=1}^{N_x} c_{ik}^{(1)} u_{0_{k,m}} \\
& + (A_3-A_1)\sum_{k=1}^{N_y} c_{jk}^{(3)} w_{i,k} + (B_3-B_1-2C_1+2C_3)\sum_{m=1}^{N_y} c_{jm}^{(1)}\sum_{k=1}^{N_x} c_{ik}^{(2)} w_{k,m} \\
& + C_3\sum_{k=1}^{N_x} c_{ik}^{(2)}\varphi_{y_{k,j}} + A_3\sum_{k=1}^{N_y} c_{jk}^{(2)}\varphi_{y_{i,k}} + (B_3+C_3)\sum_{m=1}^{N_y} c_{jm}^{(1)}\sum_{k=1}^{N_x} c_{ik}^{(1)}\varphi_{x_{k,m}} \\
= {} & I_0\ddot{v}_0 + (I_3-I_1)\sum_{k=1}^{N_y} c_{jk}^{(1)}\ddot{w}_{i,k} + I_3\ddot{\varphi}_y - L_0\sum_{k=1}^{N_x} c_{ik}^{(2)}\ddot{v}_{0_{k,j}} \\
& - (L_3-L_1)\sum_{k=1}^{N_y} c_{jk}^{(3)}\ddot{w}_{i,k} - L_3\sum_{k=1}^{N_x} c_{ik}^{(2)}\ddot{\varphi}_{y_{k,j}} - L_0\sum_{k=1}^{N_y} c_{jk}^{(2)}\ddot{v}_{0_{i,k}} \\
& - (L_3-L_1)\sum_{m=1}^{N_y} c_{jm}^{(1)}\sum_{k=1}^{N_x} c_{ik}^{(2)}\ddot{w}_{k,m} - L_3\sum_{k=1}^{N_y} c_{jk}^{(2)}\ddot{\varphi}_{y_{i,k}},
\end{aligned}
$$

$$
\begin{aligned}
(\mathrm{A3}) \quad & (A_1 - A_3)\Big(\sum_{k=1}^{N_y} c_{jk}^{(3)} v_{0_{i,k}} + \sum_{k=1}^{N_x} c_{ik}^{(3)} u_{0_{k,j}}\Big) \\
& + (2A_4 - A_2 - A_5)\Big(\sum_{k=1}^{N_x} c_{ik}^{(4)} w_{k,j} + \sum_{k=1}^{N_y} c_{jk}^{(4)} w_{i,k}\Big) \\
& + (A_4 - A_5)\Big(\sum_{k=1}^{N_x} c_{ik}^{(3)} \varphi_{x_{k,j}} + \sum_{k=1}^{N_y} c_{jk}^{(3)} \varphi_{y_{i,k}}\Big) \\
& + (B_1 - B_3 + 2C_1 - 2C_3)\Big(\sum_{m=1}^{N_y} c_{jm}^{(1)} \sum_{k=1}^{N_x} c_{ik}^{(2)} v_{0_{k,m}} + \sum_{m=1}^{N_y} c_{jm}^{(2)} \sum_{k=1}^{N_x} c_{ik}^{(1)} u_{0_{k,m}}\Big) \\
& + 2(2B_4 - B_2 - B_5 + 4C_4 - 2C_2 - 2C_5) \sum_{m=1}^{N_y} c_{jm}^{(2)} \sum_{k=1}^{N_x} c_{ik}^{(2)} w_{k,m} \\
& + (B_4 - B_5 + 2C_4 - 2C_5)\Big(\sum_{m=1}^{N_y} c_{jm}^{(1)} \sum_{k=1}^{N_x} c_{ik}^{(2)} \varphi_{y_{k,m}} + \sum_{m=1}^{N_y} c_{jm}^{(2)} \sum_{k=1}^{N_x} c_{ik}^{(1)} \varphi_{x_{k,m}}\Big) \\
& + C_6\Big(\sum_{k=1}^{N_x} c_{ik}^{(1)} \varphi_{x_{k,j}} + \sum_{k=1}^{N_y} c_{jk}^{(1)} \varphi_{y_{i,k}}\Big) + C_6\Big(\sum_{k=1}^{N_x} c_{ik}^{(2)} w_{k,j} + \sum_{k=1}^{N_y} c_{jk}^{(2)} w_{i,k}\Big) \\
= {} & I_0 \ddot{w} + (I_1 - I_3)\Big(\sum_{k=1}^{N_x} c_{ik}^{(1)} \ddot{u}_{0_{k,j}} + \sum_{k=1}^{N_y} c_{jk}^{(1)} \ddot{v}_{0_{i,k}}\Big) \\
& + (-I_2 + 2I_4 - I_5)\Big(\sum_{k=1}^{N_x} c_{ik}^{(2)} \ddot{w}_{k,j} + \sum_{k=1}^{N_y} c_{jk}^{(2)} \ddot{w}_{i,k}\Big) \\
& + (I_4 - I_5)\Big(\sum_{k=1}^{N_x} c_{ik}^{(1)} \ddot{\varphi}_{x_{k,j}} + \sum_{k=1}^{N_y} c_{jk}^{(1)} \ddot{\varphi}_{y_{i,k}}\Big) \\
& - L_0 \sum_{k=1}^{N_x} c_{ik}^{(2)} \ddot{w}_{k,j} - (L_1 - L_3)\Big(\sum_{k=1}^{N_x} c_{ik}^{(3)} \ddot{u}_{0_{k,j}} + \sum_{m=1}^{N_y} c_{jm}^{(1)} \sum_{k=1}^{N_x} c_{ik}^{(2)} \ddot{v}_{0_{k,m}}\Big) \\
& - (-L_2 + 2L_4 - L_5)\Big(\sum_{k=1}^{N_x} c_{ik}^{(4)} \ddot{w}_{k,j} + \sum_{m=1}^{N_y} c_{jm}^{(2)} \sum_{k=1}^{N_x} c_{ik}^{(2)} \ddot{w}_{k,m}\Big) \\
& - (L_4 - L_5)\Big(\sum_{k=1}^{N_x} c_{ik}^{(3)} \ddot{\varphi}_{x_{k,j}} + \sum_{m=1}^{N_y} c_{jm}^{(1)} \sum_{k=1}^{N_x} c_{ik}^{(2)} \ddot{\varphi}_{y_{k,m}}\Big) \\
& - L_0 \sum_{k=1}^{N_y} c_{jk}^{(2)} \ddot{w}_{i,k} - (L_1 - L_3)\Big(\sum_{m=1}^{N_y} c_{jm}^{(2)} \sum_{k=1}^{N_x} c_{ik}^{(1)} \ddot{u}_{0_{k,m}} + \sum_{k=1}^{N_y} c_{jk}^{(3)} \ddot{v}_{0_{i,k}}\Big)
\end{aligned}
$$

$$
\begin{aligned}
&- (-L_2 + 2L_4 - L_5)\Big(\sum_{m=1}^{N_y} c_{jm}^{(2)} \sum_{k=1}^{N_x} c_{ik}^{(2)} \ddot{w}_{k,m} + \sum_{k=1}^{N_y} c_{jk}^{(4)} \ddot{w}_{i,k}\Big) \\
&- (L_4 - L_5)\Big(\sum_{m=1}^{N_y} c_{jm}^{(2)} \sum_{k=1}^{N_x} c_{ik}^{(1)} \ddot{\varphi}_{x_{k,m}} + \sum_{k=1}^{N_y} c_{jk}^{(3)} \ddot{\varphi}_{y_{i,k}}\Big),
\end{aligned}
$$

$$
\begin{aligned}
\text{(A4)}\quad & A_3 \sum_{k=1}^{N_x} c_{ik}^{(2)} u_{0_{k,j}} + C_3 \sum_{k=1}^{N_y} c_{jk}^{(2)} u_{0_{i,k}} + (B_3 + C_3) \sum_{m=1}^{N_y} c_{jm}^{(1)} \sum_{k=1}^{N_x} c_{ik}^{(1)} v_{0_{k,m}} \\
&+ (A_5 - A_4)_3 \sum_{k=1}^{N_x} c_{ik}^{(3)} w_{k,j} + (B_5 - B_4 - 2C_4 + 2C_5) \sum_{m=1}^{N_y} c_{jm}^{(2)} \sum_{k=1}^{N_x} c_{ik}^{(1)} w_{k,m} \\
&+ A_5 \sum_{k=1}^{N_x} c_{ik}^{(2)} \varphi_{x_{k,j}} + C_5 \sum_{k=1}^{N_y} c_{jk}^{(2)} \varphi_{x_{i,k}} + (B_5 + C_5) \sum_{m=1}^{N_y} c_{jm}^{(1)} \sum_{k=1}^{N_x} c_{ik}^{(1)} \varphi_{y_{k,m}} \\
&- C_6 \varphi_x - C_6 \sum_{k=1}^{N_x} c_{ik}^{(1)} w_{k,j} \\
= {} & I_3 \ddot{u}_0 + (I_5 - I_4) \sum_{k=1}^{N_x} c_{ik}^{(1)} \ddot{w}_{k,j} + I_5 \ddot{\varphi}_x - L_3 \sum_{k=1}^{N_x} c_{ik}^{(2)} \ddot{u}_{0_{k,j}} \\
&- (L_5 - L_4) \sum_{k=1}^{N_x} c_{ik}^{(3)} \ddot{w}_{k,j} - L_5 \sum_{k=1}^{N_x} c_{ik}^{(2)} \ddot{\varphi}_{x_{k,j}} - L_3 \sum_{k=1}^{N_y} c_{jk}^{(2)} \ddot{u}_{0_{i,k}} \\
&- (L_5 - L_4) \sum_{m=1}^{N_y} c_{jm}^{(2)} \sum_{k=1}^{N_x} c_{ik}^{(1)} \ddot{w}_{k,m} - L_5 \sum_{k=1}^{N_y} c_{jk}^{(2)} \ddot{\varphi}_{x_{i,k}},
\end{aligned}
$$

$$
\begin{aligned}
\text{(A5)}\quad & C_3 \sum_{k=1}^{N_x} c_{ik}^{(2)} v_{0_{k,j}} + A_3 \sum_{k=1}^{N_y} c_{jk}^{(2)} v_{0_{i,k}} + (B_3 + C_3) \sum_{m=1}^{N_y} c_{jm}^{(1)} \sum_{k=1}^{N_x} c_{ik}^{(1)} u_{0_{k,m}} \\
&+ (A_5 - A_4) \sum_{k=1}^{N_y} c_{jk}^{(3)} w_{i,k} + (B_5 - B_4 - 2C_4 + 2C_5) \sum_{m=1}^{N_y} c_{jm}^{(1)} \sum_{k=1}^{N_x} c_{ik}^{(2)} w_{k,m} \\
&+ C_5 \sum_{k=1}^{N_x} c_{ik}^{(2)} \varphi_{y_{k,j}} + A_5 \sum_{k=1}^{N_y} c_{jk}^{(2)} \varphi_{y_{i,k}} + (B_5 + C_5) \sum_{m=1}^{N_y} c_{jm}^{(1)} \sum_{k=1}^{N_x} c_{ik}^{(1)} \varphi_{x_{k,m}} \\
&- C_6 \varphi_y - C_6 \sum_{k=1}^{N_y} c_{jk}^{(1)} w_{i,k}
\end{aligned}
$$

$$= I_3\ddot{v}_0 + (I_5 - I_4)\sum_{k=1}^{N_y} c_{jk}^{(1)}\ddot{w}_{i,k} + I_5\ddot{\varphi}_y - L_3\sum_{k=1}^{N_x} c_{ik}^{(2)}\ddot{v}_{0_{k,j}}$$
$$- (L_5 - L_4)\sum_{k=1}^{N_y} c_{jk}^{(3)}\ddot{w}_{i,k} - L_5\sum_{k=1}^{N_x} c_{ik}^{(2)}\ddot{\varphi}_{y_{k,j}} - L_3\sum_{k=1}^{N_y} c_{jk}^{(2)}\ddot{v}_{0_{i,k}}$$
$$- (L_5 - L_4)\sum_{m=1}^{N_y} c_{jm}^{(1)}\sum_{k=1}^{N_x} c_{ik}^{(2)}\ddot{w}_{k,m} - L_5\sum_{k=1}^{N_y} c_{jk}^{(2)}\ddot{\varphi}_{y_{i,k}}.$$

$N_x$ and $N_y$ above are number of nodal points in $x$- and $y$-directions, respectively, and $A_j$, $B_j$, and $C_j$ are expressed by Eq. (3.9).

## References


1. Y. Fu, H. Du, S. Zhang, *Functionally graded TiN/TiNi shape memory alloy films*, Mater. Lett., **57**, 2995–2999, 2003.
2. A.M.A. Witvrouw, A. Mehta, *The use of functionally graded poly-SiGe layers for MEMS application*, Mater. Sci. Forum., **492–493**, 255–260, 2005.
3. H. Hassanin, K. Jiang, *Net shape manufacturing of ceramic micro parts with tailored graded layers*, J. Micromechanics Microengineering, **24**, Paper No.: 015018, 2014.
4. A.C. Eringen, D.G.B. Edelen, *On nonlocal elasticity*, Int. J. Eng. Sci., **10**, 233–248, 1972.
5. A.C. Eringen, *Nonlocal polar elastic continua*, Int. J. Eng. Sci., **10**, 1–16, 1972.
6. E.C. Aifantis, *Strain gradient interpretation of size effects*, Int. J. Fracture, **95**, 299–314, 1999.
7. N.A. Fleck, J.W. Hutchinson, *Strain gradient plasticity*, [in:] W.H. John, Y.W. Theodore (Eds.), Advances in Applied Mechanics, **33**, 299–314, 1997.
8. N.A. Fleck, J.W. Hutchinson, *A reformulation of strain gradient plasticity*, J. Mech. Phys. Solids, **49**, 2245–2271, 2001.
9. D.C.C. Lam, F. Yang, A.C.M. Chong, J. Wang, P. Tong, *Experiments and theory in strain gradient elasticity*, J. Mech. Phys. Solids, **51**, 1477–1508, 2003.
10. R.D. Mindlin, H.F. Tiersten, *Effects of couple-stresses in linear elasticity*, Arch. Ration. Mech. Anal., **11**, 415–448, 1962.
11. F. Yang, A.C.M. Chong, D.C.C. Lam, P. Tong, *Couple stress based strain gradient theory for elasticity*, Int. J. Solids Struct., **39**, 2731–2743, 2002.
12. I. Eshraghi, S. Dag, N. Soltani, *Bending and free vibrations of functionally graded annular and circular micro-plates under thermal loading*, Compos. Struct., **137**, 196–207, 2016.
13. O. Rahmani, O. Pedram, *Analysis and modeling the size effect on vibration of functionally graded nanobeams based on nonlocal Timoshenko beam theory*, Int. J. Eng. Sci., **77**, 55–70, 2014.

14. F. Ebrahimi, M. Barati, *A nonlocal higher-order shear deformation beam theory for vibration analysis of size-dependent functionally graded nanobeams*, Arab. J. Sci. Eng., **41**, 1–12, 2015.

15. M. Şimşek, H.H. Yurtcu, *Analytical solutions for bending and buckling of functionally graded nanobeams based on the nonlocal Timoshenko beam theory*, Compos. Struct., **97**, 378–386, 2013.

16. O. Rahmani, A.A. Jandaghian, *Buckling analysis of functionally graded nanobeams based on a nonlocal third-order shear deformation theory*, Appl. Phys. A., **119**, 1019–1032, 2015.

17. R. Nazemnezhad, S. Hosseini-Hashemi, *Nonlocal nonlinear free vibration of functionally graded nanobeams*, Compos. Struct., **110**, 192–199, 2014.

18. S. Hosseini-Hashemi, R. Nazemnezhad, M. Bedroud, *Surface effects on nonlinear free vibration of functionally graded nanobeams using nonlocal elasticity*, Appl. Math. Model., **38**, 3538–3553, 2014.

19. B. Uymaz, *Forced vibration analysis of functionally graded beams using nonlocal elasticity*, Compos. Struct., **105**, 227–239, 2013.

20. F. Ebrahimi, E. Salari, *Nonlocal thermo-mechanical vibration analysis of functionally graded nanobeams in thermal environment*, Acta Astronaut., **113**, 29–50, 2015.

21. M.A. Eltaher, S.A. Emam, F.F. Mahmoud, *Free vibration analysis of functionally graded size-dependent nanobeams*, Appl. Math. Comput., **218**, 7406–7420, 2012.

22. M.A. Eltaher, S.A. Emam, F.F. Mahmoud, *Static and stability analysis of nonlocal functionally graded nanobeams*, Compos. Struct., **96**, 82–88, 2013.

23. M.A. Eltaher, A. Khairy, A.M. Sadoun, F.A. Omar, *Static and buckling analysis of functionally graded Timoshenko nanobeams*, Appl. Math. Comput., **229**, 283–295, 2014.

24. J.N. Reddy, S. El-Borgi, J. Romanoff, *Non-linear analysis of functionally graded microbeams using Eringen's non-local differential model*, Int. J. Nonlinear Mech., **67**, 308–318, 2014.

25. M. Zare, R. Nazemnezhad, S. Hosseini-Hashemi, *Natural frequency analysis of functionally graded rectangular nanoplates with different boundary conditions via an analytical method*, Meccanica, **50**, 2391–2408, 2015.

26. S. Natarajan, S. Chakraborty, M. Thangavel, S. Bordas, T. Rabczuk, *Size-dependent free flexural vibration behavior of functionally graded nanoplates*, Comput. Mater. Sci., **65**, 74–80, 2012.

27. M.R. Nami, M. Janghorban, *Free vibration of functionally graded size dependent nanoplates based on second order shear deformation theory using nonlocal elasticity theory*, Iran. J. Sci. Technol. Trans. Mech. Eng., **39**, 15–28, 2015.

28. A. Daneshmehr, A. Rajabpoor, A. Hadi, *Size dependent free vibration analysis of nanoplates made of functionally graded materials based on nonlocal elasticity theory with high order theories*, Int. J. Eng. Sci., **95**, 23–35, 2015.

29. A. Daneshmehr, A. Rajabpoor, M. Pourdavood, *Stability of size dependent functionally graded nanoplate based on nonlocal elasticity and higher order plate theories and different boundary conditions*, Int. J. Eng. Sci., **82**, 84–100, 2014.

30. M.R. NAMI, M. JANGHORBAN, M. DAMADAM, *Thermal buckling analysis of functionally graded rectangular nanoplates based on nonlocal third-order shear deformation theory*, Aerosp. Sci. Technol., **41**, 7–15, 2015.

31. H. KANANIPOUR, *Static analysis of nanoplates based on the nonlocal Kirchhoff and Mindlin plate theories using DQM*, Lat. Am. J. Solids Struct., **11**, 1709–1720, 2014.

32. H. SALEHIPOUR, H. NAHVI, A.R. SHAHIDI, *Closed-form elasticity solution for three-dimensional deformation of functionally graded micro/nano plates on elastic foundation*, Lat. Am. J. Solids Struct., **12**, 747–762, 2015.

33. H. SALEHIPOUR, H. NAHVI, A.R. SHAHIDI, *Exact analytical solution for free vibration of functionally graded micro/nanoplates via three-dimensional nonlocal elasticity*, Phys. E Low-Dimensional Syst. Nanostructures, **66**, 350–358, 2015.

34. R. ANSARI, M. FAGHIH SHOJAEI, A. SHAHABODINI, M. BAZDID-VAHDATI, *Three-dimensional bending and vibration analysis of functionally graded nanoplates by a novel differential quadrature-based approach*, Compos. Struct., **131**, 753–764, 2015.

35. T.J.R. HUGHES, J.A. COTTRELL, Y. BAZILEVS, *Isogeometric analysis: CAD, finite elements, NURBS, exact geometry and mesh refinement*, Comput. Method Appl. M., **194**, 4135–4195, 2005.

36. S. NATARAJAN, S. CHAKRABORTY, M. THANGAVEL, S. BORDAS, T. RABCZUK, *Size-dependent free flexural vibration behavior of functionally graded nanoplates*, Comp. Mater. Sci., **65**, 74–80, 2012.

37. N.-T. NGUYEN, D. HUI, J. LEE, H. NGUYEN-TUAN, *An efficient computational approach for size-dependent analysis of functionally graded nanoplates*, Comput. Method Appl. M., **297**, 191–218, 2015.

38. R. ANSARI, A. NOROUZZADEH, *Nonlocal and surface effects on the buckling behavior of functionally graded nanoplates: An isogeometric analysis*, Physica E: Low-dimensional Systems and Nanostructures, **84**, 84–97, 2016.

39. H. NGUYEN-XUAN, L.V. TRAN, C.H. THAI, S. KULASEGARAM, S.P.A. BORDAS, *Isogeometric analysis of functionally graded plates using a refined plate theory*, Compos. Part B: Eng., **64**, 222–234, 2014.

40. S.A. FARZAM-RAD, B. HASSANI, A. KARAMODIN, *Isogeometric analysis of functionally graded plates using a new quasi-3D shear deformation theory based on physical neutral surface*, Compos. Part B: Eng., **108**, 174–189, 2017.

41. T. YU, S. YIN, T.Q. BUI, C. LIU, N. WATTANASAKULPONG, *Buckling isogeometric analysis of functionally graded plates under combined thermal and mechanical loads*, Compos. Struct., **162**, 54–69, 2017.

42. Y. LIANG, Q. HAN, *Prediction of the nonlocal scaling parameter for graphene sheet*, Eur. J. Mech. – A/Solids, **45**, 153–160, 2014.

43. R. AGHAZADEH, E. CIGEROGLU, S. DAG, *Static and free vibration analyses of small-scale functionally graded beams possessing a variable length scale parameter using different beam theories*, Eur. J. Mech. – A/Solids, **46**, 1–11, 2014.

44. I. ESHRAGHI, S. DAG, N. SOLTANI, *Consideration of spatial variation of the length scale parameter in static and dynamic analyses of functionally graded annular and circular micro-plates*, Compos. Part B: Eng., **78**, 338–348, 2015.

45. A.C. Eringen, *On differential equations of nonlocal elasticity and solutions of screw dislocation and surface waves*, J. Appl. Phys., **54**, 4703–4710, 1983.

46. E. Ghavanloo, S.A. Fazelzadeh, *Evaluation of nonlocal parameter for single-walled carbon nanotubes with arbitrary chirality*, Meccanica, **51**, 41–54, 2016.

47. R. Ansari, S. Sahmani, *Small-scale effect on vibrational response of single-walled carbon nanotubes with different boundary conditions based on nonlocal beam models*, Commun. Nonlinear. Sci., **17**, 1965–1979, 2012.

48. R. Ansari, H. Rouhi, S. Sahmani, *Calibration of the analytical nonlocal shell model for vibrations of double-walled carbon nanotubes with arbitrary boundary conditions using molecular dynamics*, Int. J. Mech. Sci., **53**, 786–792, 2011.

49. R. Ansari, S. Sahmani, B. Arash, *Nonlocal plate model for free vibrations of single-layered graphene sheets*, Phys. Lett. A, **375**, 53–62, 2010.

50. A.M. van der Zande, R.A. Barton, J.S. Alden, C.S. Ruiz-Vargas, W.S. Whitney, P.H.Q. Pham, J. Park, J.M. Parpia, H.G. Craighead, P.L. McEuen, *Large-scale arrays of single-layer graphene resonators*, Nano Lett., **10**, 4869–4873, 2010.

51. Y. Yuasa, A. Yoshinaka, T. Arie, S. Akita, *Visualization of vibrating cantilevered multilayer graphene mechanical oscillator*, Appl. Phys. Express, **4**, Paper No.: 115103, 2011.

52. H. Du, M.K. Lim, R.M. Lin, *Application of generalized differential quadrature method to structural problems*, Int. J. Numer. Methods Eng., **37**, 1881–1896, 1994.

53. C. Shu, *Differential Quadrature and Its Application in Engineering*, Springer, London, 2012.

54. C.M. Wang, J.N. Reddy, K.H. Lee, *Shear Deformable Beams and Plates: Relationships with Classical Solutions*, Elsevier, Oxford, 2000.

*Received August 8, 2016; revised version January 23, 2017.*